TISSUE ENGINEERING: Part C
Volume 22, Number 12, 2016

DOI: 10.1089/ten.tec.2016.0345

termis
Tissue Engineering
& Regenerative Medicine
International Society

METHODS ARTICLE

Cryopreservation of Brain Endothelial Cells Derived from Human Induced Pluripotent Stem Cells Is Enhanced by Rho-Associated Coiled Coil-Containing Kinase Inhibition

Hannah K. Wilson, PhD, Madeline G. Faubion, Michael K. Hjortness, Sean P. Palecek, PhD, and Eric V. Shusta, PhD

The blood–brain barrier (BBB) maintains brain homeostasis but also presents a major obstacle to brain drug delivery. Brain microvascular endothelial cells (BMECs) form the principal barrier and therefore represent the major cellular component of *in vitro* BBB models. Such models are often used for mechanistic studies of the BBB in health and disease and for drug screening. Recently, human induced pluripotent stem cells (iPSCs) have emerged as a new source for generating BMEC-like cells for use in *in vitro* human BBB studies. However, the inability to cryopreserve iPSC-BMECs has impeded implementation of this model by requiring a fresh differentiation to generate cells for each experiment. Cryopreservation of differentiated iPSC-BMECs would have a number of distinct advantages, including enabling production of larger scale lots, decreasing lead time to generate purified iPSC-BMEC cultures, and facilitating use of iPSC-BMECs in large-scale screening. In this study, we demonstrate that iPSC-BMECs can be successfully cryopreserved at multiple differentiation stages. Cryopreserved iPSC-BMECs retain high viability, express standard endothelial and BBB markers, and reach a high transendothelial electrical resistance (TEER) of $\sim$3000 $\Omega \cdot cm^2$, equivalent to nonfrozen controls. Rho-associated coiled coil-containing kinase (ROCK) inhibitor Y-27632 substantially increased survival and attachment of cryopreserved iPSC-BMECs, as well as stabilized TEER above 800 $\Omega \cdot cm^2$ out to 7 days post-thaw. Overall, cryopreservation will ease handling and storage of high-quality iPSC-BMECs, reducing a key barrier to greater implementation of these cells in modeling the human BBB.

Keywords: blood–brain barrier, human induced pluripotent stem cells, cryopreservation, ROCK inhibitor

Introduction

The microvasculature of the central nervous system (CNS), collectively termed the blood–brain barrier (BBB), limits the free flow of substances between the blood and the brain. This barrier is responsible for maintaining brain homeostasis while also protecting the brain from potentially harmful toxins and pathogens. The importance of this barrier for proper brain function is highlighted by the severe nature of diseases where BBB function is impaired, including stroke,[1] traumatic brain injury,[2] and Alzheimer's disease.[3] The BBB also presents a substantial obstacle to CNS drug delivery, preventing many drugs from appreciably entering the brain.[4]

The BBB is lined with specialized endothelial cells (ECs) termed brain microvascular ECs (BMECs). As a result of their anatomical positioning between the bloodstream and the CNS, BMECs regulate the transport of substances into and out of the brain. BMECs are sealed together by intercellular junction proteins, including those of both adherens and tight junctions, which prevent paracellular diffusion.[5] BMECs also express a variety of transporters, including efflux transporters that limit penetration of potentially harmful substances, and nutrient transporters that influx nutrients necessary for proper brain function.[6,7] Human *in vitro* BBB models, including primary and immortalized BMECs,[8,9] recapitulate many key properties of the *in vivo* BBB; however, limited barrier properties restrict the utility of these models. Stem cells have emerged as an attractive source for generating a renewable source of human BMEC-like cells.[10–13] As one approach, our laboratory has developed methods to differentiate human induced pluripotent stem cells (iPSCs) into ECs possessing many characteristics of the *in vivo* BBB, including tight junctions, efflux transporters, and nutrient transporters.[10] Moreover, retinoic acid (RA) treatment during iPSC-BMEC

Department of Chemical and Biological Engineering, University of Wisconsin-Madison, Madison, Wisconsin.

differentiations upregulates several key attributes, most notably increased maximum transendothelial electrical resistance (TEER), which approaches *in vivo* values.[11]

Much like the *in vivo* BBB,[14] the iPSC-BMECs do not proliferate extensively following differentiation and hence cannot be readily passaged as differentiated cells. Thus, scaling iPSC-BMEC production requires expansion of the undifferentiated iPSCs followed by large-scale differentiation. Cryopreservation has been used extensively for storing both primary and immortalized BMECs from human and nonhuman sources.[9,15] In particular, primary porcine BMECs have been shown to retain BBB properties up to at least 8–12 months after cryopreservation following initial isolation.[16,17] In addition, iPSC-derived cell types such as cardiomyocytes, retinal pigment epithelium, and neural progenitor cells have also been successfully cryopreserved.[18–22] Thus, to expand the utility of the iPSC-BMEC model, we sought to develop a robust cryopreservation protocol. We found that iPSC-BMECs could be cryopreserved at multiple stages of differentiation and retained excellent BMEC properties upon thaw. The addition of Rho-associated coiled coil-containing kinase (ROCK) inhibitor Y-27632 to thawed iPSC-BMECs substantially improved cell attachment and survival and also improved TEER of the cryopreserved cells. iPSC-BMECs could be cryopreserved for at least 3 months without loss of BBB properties. We expect the cryopreservation protocol will greatly enhance the utility and deployment of the iPSC-derived BBB model by streamlining the iPSC-BMEC production pipeline.

Materials and Methods

Cell culture and BMEC differentiation

For detailed methods of iPSC-BMEC differentiation see Ref.[23] Briefly, IMR90-4[24] and CS03iCTRn2 iPSCs were maintained in feeder-free conditions on Matrigel (BD Biosciences) in mTeSR1 media (WiCell Research Institute). CS03iCTRn2 iPSCs were reprogrammed from fibroblasts from a healthy subject by transfecting with nonintegrating episomal plasmids expressing *OCT4, SOX2, C-MYC*, and *KLF4*. Successful reprogramming was verified by immunocytochemistry for the pluripotency markers Nanog, TRA160, Oct4, SSEA4, TRA181, and Sox2, as well as the activity of the pluripotency marker alkaline phosphatase. In addition, G-band karyotype analysis confirmed that the line showed no chromosomal abnormalities. All experiments were performed using IMR90-4 iPSCs between passages 36 and 70 and CS03iCTRn2 iPSCs between passages 48 and 64. For routine maintenance, iPSCs were passaged with Versene (Life Technologies) every 4–5 days. For passaging before differentiation, iPSCs were dissociated with cold Accutase (Innovative Cell Technologies) for 7 min, and the number of live cells was quantified using a hemocytometer with Trypan blue staining (Life Technologies). Single-cell suspensions of iPSCs were seeded with 10 μM Y-27632 (Tocris Bioscience) at a density between 8000 and 15,000 cells/cm^2. After 24 h, Y-27632 was withdrawn and cells were refed mTeSR1 every 24 h for two additional days. Immediately before initiating differentiation, the density of a single well was quantified using a hemocytometer to ensure that the day 0 iPSC starting density was within the range of 30,000 ± 10,000 cells/cm^2.[25] To initiate differentiation, the remaining wells were switched to unconditioned medium (UM): DMEM/F12 (Life Technologies) with 20% KnockOut Serum Replacement (Life Technologies), 1× MEM nonessential amino acids (Life Technologies), 1 mM GlutaMAX (Life Technologies), and 0.1 mM β-mercaptoethanol (Sigma). Cells were refed UM every 24 h for 6 days, followed by 2 days in EC medium supplemented with RA: hESFM (Life Technologies) with 1% platelet poor plasma-derived serum (PDS; Fisher Scientific), 20 ng/mL bFGF (Waisman Biomanufacturing), and 10 μM RA (Sigma) diluted in DMSO (Sigma). The final concentration of DMSO in the RA-containing EC media was 0.1%. Medium was not changed during the EC treatment phase (D6–D8). Routine purification of iPSC-BMECs was accomplished through selective adhesion. At D8 of differentiation, cells were subcultured onto collagen IV/fibronectin-coated polystyrene plates (Costar) or 0.4 μm 12-well polyester Transwells (Costar). The coating concentrations used for Transwell filters were 0.4 mg/mL collagen IV (Sigma) and 0.1 mg/mL fibronectin (Sigma) in water, and this solution was diluted 5× for coating polystyrene plates. Cells were subcultured into EC+RA medium, and after 24 h (i.e., D9 of differentiation), the medium was switched to hESFM +1% PDS (removing dead cells and withdrawing bFGF and RA). Medium was not changed thereafter. Differentiations that achieved a maximum TEER of at least 1500 Ω·cm^2 were considered high quality and used for cryopreservation experiments.

Cryopreservation of iPSC-BMECs

Cells were cryopreserved at either D8 of differentiation (before purification) or at D10 of differentiation (as purified BMECs), and the cryopreservation protocol was the same for each. Cells were dissociated with Accutase for 15–45 min (i.e., until a single-cell suspension was formed) and quantified using a hemocytometer with Trypan blue staining. Single cells were resuspended in freezing medium (10% DMSO and 30% fetal bovine serum [Life Technologies] in EC medium), transferred to cryotubes (Thermo Scientific), and placed in an isopropanol container overnight at −80°C. The next day, tubes were transferred to a liquid nitrogen tank and remained in the cryostorage for at least 24 h before thawing, if not otherwise specified.

Thawing iPSC-BMECs

The thawing procedure was the same for iPSC-BMECs cryopreserved at D8 and D10 of differentiation. Tissue culture plates and Transwells were coated with collagen IV/fibronectin as described for nonfrozen cells. Frozen cells were thawed rapidly in a 37°C water bath, resuspended in EC+RA medium (with or without 10 μM Y-27632), and quantified using a hemocytometer with Trypan blue stain. Cells were seeded at a density of 1 million cells/cm^2 on 12-well Transwell filters or 0.5–1 million cells/cm^2 in tissue culture plates. After 24 h post-thaw, culture medium was changed to hESFM with 1% PDS, with or without 10 μM Y-27632. Medium was not changed thereafter. For CS03iCTRn2 iPSC-BMECs, media exchanges were performed at 6 and 24 h post-thaw to remove nonadherent cells to maximize TEER.

Cell viability and yield

Viability was measured using Trypan blue staining. For cell yield measurement, 0.5 million cells/cm^2 were seeded

into 24-well plates. After the designated length of time, the supernatant was removed and the adherent cells were gently washed 1× with phosphate-buffered saline (PBS). Adherent cells were dissociated with Accutase and quantified using a hemocytometer with Trypan blue stain. Cell yield was quantified as the number of viable attached cells divided by the number of viable cells initially seeded.

TEER measurement

TEER was measured through EVOM voltohmmeter with STX2 electrodes (World Precision Instruments), and all measurements were performed at 37°C to prevent fluctuations in TEER value due to temperature change. The resistance value of an empty filter coated with collagen IV/fibronectin was subtracted from each measurement.

Quantitative polymerase chain reaction

For RNA extraction, cells were washed 1× with PBS and dissociated with Accutase. Total RNA was extracted using RNEasy Mini kit (Qiagen) according to the manufacturer's instructions. cDNA was generated from 1 μg total RNA using Omniscript reverse transcriptase (Qiagen) and oligo-dT primers (Invitrogen). Quantitative polymerase chain reaction (qPCR) was performed using 1 μL cDNA and the QuantiTect SYBR Green PCR kit (Qiagen) on an iCycler (Bio-Rad). Primer sequences used are summarized in Supplementary Table S1 (Supplementary Data are available online at www.liebertpub.com/tec). Relative expression was quantified using the comparative cycle threshold (C_T) method, normalizing to β-actin expression. Transcript amplification was analyzed by 2% agarose gel electrophoresis of the qPCR products.

Immunocytochemistry

Cells were fixed in either 100% ice-cold methanol or 4% paraformaldehyde (PFA) in PBS (Sigma) for 15 min at room temperature, washed three times with PBS, and blocked for 30 min with 10% goat serum (Sigma) in PBS. Cells were incubated with primary antibody diluted in 10% goat serum overnight at 4°C on a rocking platform (Supplementary Table S2). Cells were washed three times with PBS and incubated with goat anti-mouse or goat anti-rabbit Alexa Fluor 488 (Life Technologies) in 10% goat serum. Cell nuclei were labeled with 4′,6-diamidino-2-phenylindole dihydrochloride (DAPI; Sigma) for 10 min. Cells were washed three times with PBS and visualized. Phalloidin staining was performed on PFA-fixed cells without blocking. Alexa Fluor 594 phalloidin (Thermo Scientific) was incubated 1:20 in PBS for 30 min followed by 10-min DAPI staining. Cells were then washed three times with PBS and visualized.

Western blot

Cells were washed 1× with PBS and lysed with RIPA buffer (Pierce). Protein concentration was measured through the BCA assay (Pierce), and proteins were resolved by sodium dodecyl sulfate–polyacrylamide gel electrophoresis (SDS-PAGE) on 4–12% Tris-Glycine gels (Life Technologies). Proteins were transferred to a nitrocellulose membrane and blocked for 1 h in Tris-buffered saline (10 mM Tris-HCl, 100 mM NaCl, pH 7.5) containing 0.1% Tween-20 (TBST) and 5% milk. Membranes were probed overnight at 4°C with mouse anti-VE-cadherin (1:250; Santa Cruz), mouse anti-claudin-5 (1:250; Life Technologies), mouse anti-occludin (1:500; Life Technologies), or mouse anti ZO-1 (1:500; Life Technologies) and colabeled with rabbit anti-β-actin (1:1000; Cell Signaling Technologies) diluted in 5% milk in TBST. After five washes with TBST, membranes were incubated with infrared secondary antibodies, donkey anti-mouse IRDye 800CW (1:1000), and donkey anti-rabbit IRDye 680RD (1:1000) diluted in 5% milk in TBST. After an additional five washes with TBST, membranes were imaged through the LiCor Odyssey Infrared Imaging System, and protein quantification was performed using LiCor Image Studio v2.0.

Flow cytometry

For PECAM flow cytometry, cells were dissociated with Accutase for 15–30 min and fixed for 15 min with 1% PFA. Cells were then permeabilized for 30 min with 100% ice-cold methanol at −20°C and washed twice with wash buffer: PBS containing 0.5% bovine serum albumin (Sigma) and 0.3% Triton-X 100 (Sigma). Wash buffer was used for all washes and antibody incubation steps. Cells were incubated with anti-PECAM (1:10; Thermo Scientific) overnight at 4°C on a rotating platform. The next day, cells were washed twice and incubated for 30 min with goat anti-rabbit Alexa Fluor 488 (1:200) and again washed twice. Cells were analyzed on a FACSCalibur flow cytometer.

P-glycoprotein efflux transporter activity

Efflux transporter activity was assessed through intracellular accumulation of fluorescent P-glycoprotein (P-gp) substrate rhodamine 123 (R123). Purified iPSC-BMECs at D10 of differentiation were preincubated with or without a P-gp-specific inhibitor, 10 μM Cyclosporin A (CsA; Sigma) in HBSS buffer (Life Technologies) for 1 h at 37°C on an orbital shaker. Cells were then incubated with 10 μM R123 (Sigma) with or without CsA for an additional 2 h at 37°C on an orbital shaker. Cells were washed twice with cold PBS and lysed with RIPA buffer (Pierce), and fluorescence was measured on a plate reader (485 nm excitation and 530 nm emission). Fluorescence values were normalized to protein content as measured by BCA assay (Pierce) and reported as normalized accumulation.

Statistical analysis

Student's unpaired *t*-test was used to determine statistical significance for pairwise comparisons. For comparisons across three or more treatment conditions, analysis of variance was used followed by a Tukey test to adjust for multiple comparisons. For all significance testing, a value of $p < 0.05$ was considered significant.

Results

Development of a cryopreservation protocol for iPSC-derived BMECs

In the differentiation scheme, iPSC-BMECs and neural cells codifferentiate, with iPSC-BMECs comprising ~70% of the population by day 8 (D8) of differentiation[25] (Fig. 1A). At D8, the mixed differentiating cultures are then dissociated and the iPSC-BMECs purified through selective adhesion to a collagen IV/fibronectin matrix. During this purification

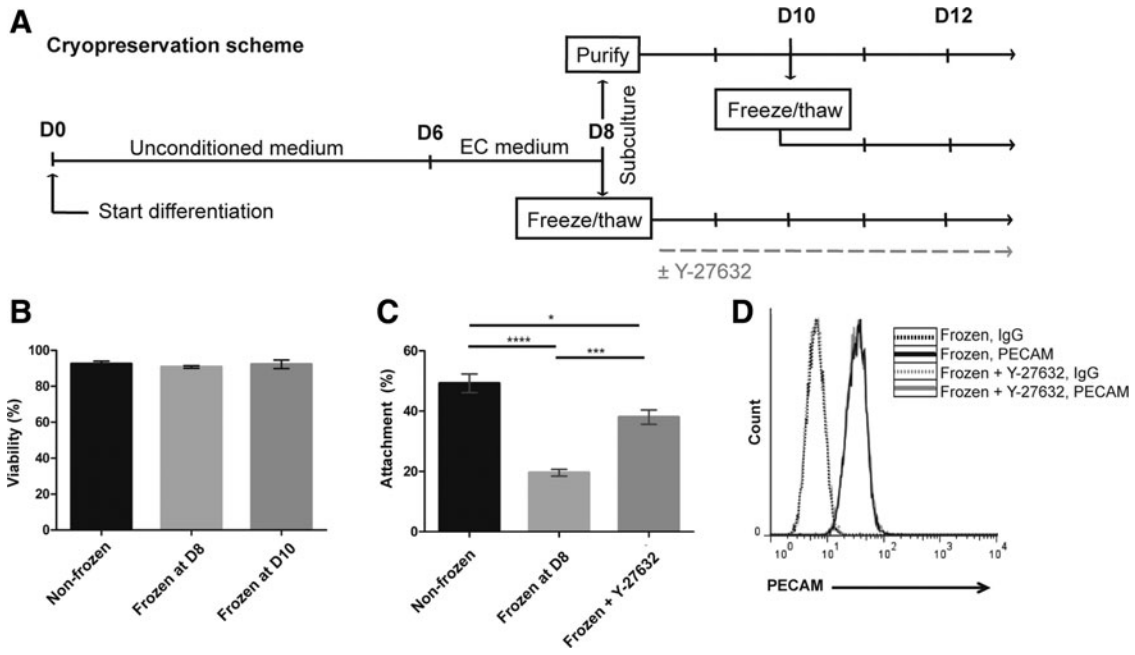

FIG. 1. Viability, yield, and purity of cryopreserved iPSC-BMECs. **(A)** Timeline of cryopreservation scheme. Cells were cryopreserved at D8 of differentiation during routine subculture or at D10 as purified iPSC-BMECs. **(B)** Viability of cryopreserved IMR90-4 iPSC-BMECs as measured by Trypan blue staining. Data are average ± standard deviation from at least three independent differentiations. **(C)** Percent attachment of cryopreserved IMR90-4 iPSC-BMECs with or without 10 μM Y-27632 treatment, calculated as the number of cells attached at 24 h post-thaw normalized to number of cells seeded at 0 h. Data represent the average ± standard deviation from triplicate samples from one independent differentiation, and experiments were repeated for an additional differentiation to verify trends. Statistical significance was calculated through ANOVA (*$p < 0.05$, ***$p < 0.001$, ****$p < 0.0001$). **(D)** Purity of cryopreserved IMR90-4 iPSC-BMECs as assessed by PECAM flow cytometry. Cells were cryopreserved at D8 of differentiation, and PECAM flow cytometry was performed 24 h post-thaw, with or without 10 μM Y-27632 treatment. ANOVA, analysis of variance; BMECs, brain microvascular endothelial cells; iPSC, induced pluripotent stem cell.

process, the iPSC-BMECs preferentially adhere to the matrix while the neural cells do not and are subsequently removed upon medium exchange (Fig. 1A). Given that the cell dissociation procedures at D8 have been optimized,[25] this was a logical differentiation stage to test cryopreservation of single-cell suspensions. Mixed D8 iPSC-derived cultures were dissociated with Accutase and cryopreserved through conventional slow-cooling techniques (see the Materials and Methods section). Following cryostorage in liquid nitrogen, cells were rapidly thawed and seeded onto collagen IV/fibronectin-coated plates. Viability of IMR90-4 iPSC-BMECs upon thaw was 91% ± 1% as assessed by Trypan blue staining, which was equivalent to Accutase-dissociated nonfrozen controls, suggesting that the freeze–thaw cycle did not induce significant cell death (Fig. 1B). In addition, cryopreserved cells were observed to proliferate with a doubling time of 14 h. However, cryopreserved cells exhibited a significant reduction in cell attachment compared to nonfrozen controls. After 24 h, cryopreserved cells yielded only a 20% ± 2% attachment compared to 49% ± 6% attachment in the nonfrozen control (Fig. 1C).

In an attempt to improve the cell attachment post-thaw, ROCK inhibitor Y-27632, which is commonly used to aid survival and attachment of undifferentiated cryopreserved iPSCs,[26,27] was tested. Addition of 10 μM Y-27632 post-thaw (Fig. 1A) substantially increased the recovery of IMR90-4 iPSC-BMECs to 38% ± 5% at 24 h (Fig. 1C). To determine whether the improved cellular yield at 24 h was the result of increased attachment rather than differential rates of proliferation, cell number was also quantified at 6 and 12 h, and no significant increases in cell number were observed for either frozen or frozen plus Y-27632 conditions (Supplementary Fig. S1). Thus, Y-27632 appears to improve cellular yield following cryopreservation through increased attachment.

The differentiation cultures frozen at D8 contained a mixture of neural and ECs.[10] Thus, to determine the purity of thawed and plated iPSC-BMECs in the recovered population, the cells were analyzed by flow cytometry for the EC marker PECAM. At 24 h post-thaw, 98% of the cells were PECAM+, suggesting that the selective adhesion-based purification process was not affected by cryopreservation (Fig. 1D). In addition, Y-27632 treatment did not affect iPSC-BMEC purity, which also yielded 98% PECAM-expressing cells. These results suggest that purified iPSC-BMEC cultures can be readily obtained following cryopreservation of the mixed differentiating D8 cultures through selective adhesion.

We also investigated the feasibility of cryopreserving purified iPSC-BMECs at D10 of differentiation, 2 days after purification (Fig. 1A). Purified IMR90-4 iPSC-BMECs retained excellent viability upon thaw (92% ± 4%, Fig. 1B) and were able to attach and form confluent monolayers. However, the yield of iPSC-BMECs recovered 2 days post-thaw after cryopreserving at D10 was lower than cryopreserving at D8. D10 cryopreservation yielded 10.6 ± 1.4 iPSC-BMECs per input undifferentiated iPSC, compared with 20.1 ± 6.2, iPSC-BMECs for D8 cryopreservation. Thus, cryopreservation at D8 at the

time of routine subculture is more efficient in that it will yield an increased number of iPSC-BMECs compared with cryopreservation of purified BMECs at D10.

Phenotypic characterization of freeze–thawed BMECs

We next tested whether BBB properties were retained in freeze–thawed iPSC-BMECs, as well as the effect of Y-27632 treatment on resultant BBB properties. IMR90-4 iPSC-BMECs cryopreserved at D8 expressed endothelial and BBB-specific markers as previously described for the nonfrozen controls (Fig. 2A and Ref.[25]). EC markers PECAM and VE-cadherin, glucose transporter Glut-1, tight junction proteins claudin-5, occludin, and ZO-1, and efflux transporters MRP1, BCRP, and P-gp were expressed in cryopreserved cells. In addition, Y-27632-treated cells

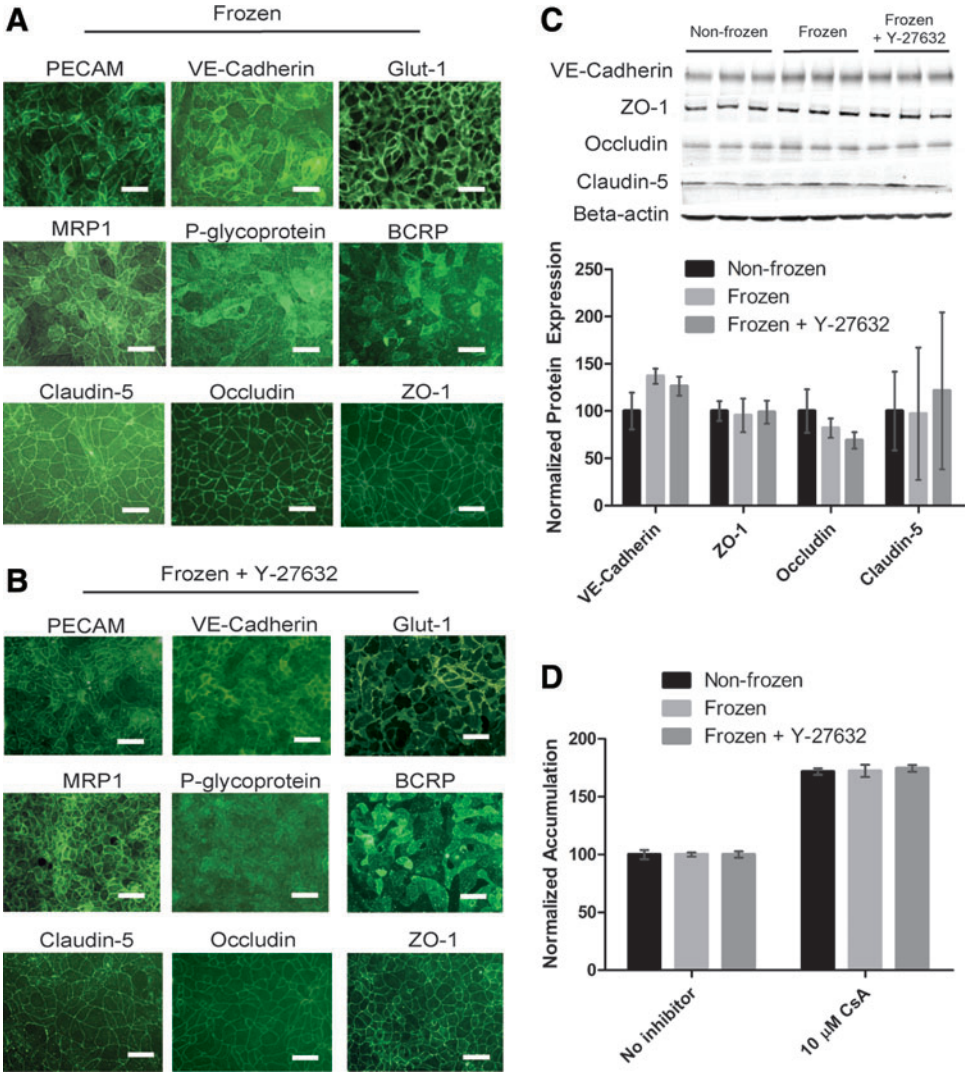

FIG. 2. BBB properties of cryopreserved iPSC-BMECs. **(A)** Immunocytochemistry of BBB markers in cryopreserved IMR90-4 iPSC-BMECs. Cells were cryopreserved at D8 of differentiation, and immunocytochemistry was performed at D10, 2 days post-thaw. Scale bars, 50 μm. **(B)** Immunocytochemistry of IMR90-4 iPSC-BMECs treated with Y-27632. Cells were cryopreserved at D8 of differentiation and treated with 10 μM Y-27632 from D8–D10. Immunocytochemistry was performed on D10 of differentiation, 2 days post-thaw. Scale bars, 50 μm. **(C)** Western blot of endothelial and tight junction proteins. IMR90-4 iPSC-BMECs were subcultured and/or cryopreserved at D8 of differentiation, and lysates were harvested at D10. Where indicated, Y-27632 (10 μM) was present D8–D10. Protein expression was normalized to β-actin, and frozen samples were paired to nonfrozen samples from the same differentiation. Data represent the average ± standard error of the mean of two independent differentiations. A representative blot from one independent differentiation with technical triplicates is shown. Lane 1–3, nonfrozen; lane 4–6, frozen; lane 7–9, frozen +10 μM Y-27632 (treated D8–D10). **(D)** P-glycoprotein activity as measured through rhodamine 123 accumulation with and without cyclosporin A (CsA) inhibition. IMR90-4 iPSC-BMECs were cryopreserved at D8 of differentiation, and the accumulation assay was performed at D10, 2 days post-thaw. Y-27632 (10 μM) was present D8–D10. RFU values were normalized to protein content and self-normalized to no inhibitor condition. Data represent the average ± standard deviation of triplicate samples from one independent differentiation, and experiments were repeated for an additional differentiation to verify trends. BBB, blood–brain barrier. Color images available online at www.liebertpub.com/tec

also maintained expression of BBB markers (Fig. 2B). Cryopreservation of purified iPSC-BMECs at D10 also yielded cells that expressed BBB markers (Supplementary Fig. S2). Similar expression of BBB markers was also observed in frozen and thawed iPSC-BMECs differentiated from CS03iCTRn2 cells (Supplementary Fig. S3).

Next, to better quantify potential freeze–thaw effects, the expression of a panel of 12 BBB genes in frozen versus nonfrozen cells was evaluated and revealed that the freezing process did not substantially change gene expression in IMR90-4 iPSC-BMECs (Supplementary Fig. S4). Transcripts for *AGER* and *ZO-1* showed a slight but statistically significant downregulation in cryopreserved BMECs ($\Delta\Delta C_t \geq -1.0$), while *LDLR* showed an increase in gene expression, although again the magnitude was small ($\Delta\Delta C_t = 0.74 \pm 0.20$). Other genes, including *BCRP*, *GLUT1*, *INSR*, *MRP1*, *OCCL*, *PGP*, *STRA6*, *TFRC*, and *VECAD* showed no statistically significant difference between frozen and nonfrozen cells ($p > 0.05$). In addition, neither were significant changes in junctional protein expression observed for VE-Cadherin, ZO-1, occludin, or claudin-5 between frozen and nonfrozen samples nor did Y-27632 treatment affect protein expression (Fig. 2C).

We further tested the potential effects of cryopreservation on P-gp efflux transporter functionality through intracellular accumulation of the P-gp substrate R123 in the presence and absence of the P-gp inhibitor CsA. The same levels of inhibition were observed between cryopreserved iPSC-BMECs and nonfrozen control cells, demonstrating that P-gp function is maintained in cryopreserved iPSC-BMECs (Fig. 2D). Furthermore, Y-27632 treatment did not affect the level of inhibition.

TEER of cryopreserved iPSC-derived BMECs

Next, TEER was measured to evaluate barrier formation in cryopreserved iPSC-BMECs. Examination of cryopreserved iPSC-BMECs and nonfrozen controls for five individual differentiations revealed that cryopreserved IMR90-4 iPSC-BMECs often had statistically significant changes in maximum TEER (either increased or decreased) compared to the nonfrozen control (Fig. 3A), but maximum TEER in all cases was in excess of 2000 $\Omega \cdot cm^2$. When collectively analyzed over five independent differentiations, IMR90-4 iPSC-BMECs cryopreserved at D8 achieved an average maximum TEER of 3150 ± 910 $\Omega \cdot cm^2$, a barrier that did not differ statistically from that of nonfrozen iPSC-BMECs, which had an average maximum TEER of 3460 ± 630 $\Omega \cdot cm^2$ ($n = 5$ independent differentiations, $p > 0.05$, Fig. 3A). Similarly, CS03iCTRn2 iPSC-BMECs frozen at D8 reached a maximum TEER of 2900 ± 1480 $\Omega \cdot cm^2$, compared to 2880 ± 1470 $\Omega \cdot cm^2$ for nonfrozen controls ($p > 0.05$, $n = 8$ independent differentiations, Supplementary Fig. S5). If instead, IMR90-4 iPSC-BMECs were cryopreserved at D10 as a purified population, TEER values of 2660 ± 1580 $\Omega \cdot cm^2$ were achieved, again indistinguishable from that of the nonfrozen controls (2790 ± 470 $\Omega \cdot cm^2$, $p > 0.05$, $n = 3$ differentiations, Supplementary Fig. S6).

Next, the effects of cryostorage duration were examined. IMR90-4 iPSC-BMECs frozen at D8 of differentiation were cryopreserved for 3 months without affecting maximum TEER (Fig. 3B). When iPSC-BMECs were frozen for 1 year, a decrease in maximum TEER was observed ($43\% \pm 38\%$ of nonfrozen controls, $p < 0.05$), suggesting that prolonged cryopreservation time is detrimental to barrier function.

The TEER of nonfrozen iPSC-BMECs typically peaks 2 days post-purification to between 2500 and 3500 $\Omega \cdot cm^2$ and then plateaus at roughly 1500 $\Omega \cdot cm^2$ by day 3–4 (Fig. 3C and Ref.[10]). Maximum TEER values were achieved 48 h post-thaw for both the nonfrozen and cryopreserved cells (Fig. 3C and Supplementary Figs. S5 and S6). While maximum TEER in cryopreserved iPSC-BMECs at 48 h post-thaw was close to that of nonfrozen controls (Fig. 3A), cryopreserved iPSC-BMECs had dramatically lower TEER at later time points compared to the controls (Fig. 3C). TEER of cryopreserved iPSC-BMECs continued to decline well below 1000 $\Omega \cdot cm^2$ after 3 days post-thaw (Fig. 3C), potentially limiting their use at later time points if high TEER is required.

Y-27632 treatment increases TEER

As a possible solution to rapid TEER decline in cryopreserved iPSC-BMECs, Transwell filter cell seeding density was first examined. We previously showed that a decrease in filter seeding density from 1 million to 0.7 million cells/cm^2 significantly decreased TEER at later time points (3–7 days post-seeding) without affecting maximum TEER at 48 h.[25] However, increasing the filter seeding density of cryopreserved IMR90-4 iPSC-BMECs did not rescue the precipitous drop in TEER, even when the density was increased threefold (3 million cells/cm^2, Supplementary Fig. S7).

Since Y-27632 treatment was useful in increasing the yield of cryopreserved iPSC-BMECs without affecting protein expression or efflux transporter function, the effects of Y-27632 on barrier function were next explored. Y-27632 has also been shown to extensively regulate EC permeability through RhoA/ROCK signaling,[28] and thus, optimizing the timing of Y-27632 addition to thawed cultures may be critical to maximizing barrier function. First, the effects of 24 h Y-27632 exposure were compared to extended exposure where Y-27632 was not withdrawn. Extended Y-27632 treatment boosted the maximum TEER compared to only adding Y-27632 for the first 24 h post-thaw (Fig. 3C, $p < 0.01$). Furthermore, both modes of Y-27632 treatment significantly increased the TEER of D8 cryopreserved iPSC-BMECs between day 3 and 6 post-thaw, maintaining TEER above 800 $\Omega \cdot cm^2$ (Fig. 3C, $p < 0.01$). Finally, extended Y-27632 treatment also reversed the detrimental effects of prolonged cryostorage, restoring the maximum TEER of D8 BMECs cryopreserved for 1 year to $97\% \pm 2\%$ of nonfrozen controls (Fig. 3B, $p < 0.05$). Therefore, Y-27632 treatment can stabilize TEER out to 7 days post-thaw as well as rescue the maximum TEER of cells cryopreserved for extended periods of time (i.e., up to 1 year).

Since a threefold increase in Transwell filter cell seeding density did not recover the nonfrozen TEER profile in cryopreserved cells (Supplementary Fig. S7), the TEER enhancing effects of Y-27632 are likely not simply the result of improved attachment (e.g., Fig. 1C). To determine the potential alternative routes by which Y-27632 might affect TEER, we analyzed expression and localization of tight junction proteins at 2 and 4 days post-thaw. No qualitative differences in occludin, claudin-5, or ZO-1 localization were observed between cryopreserved IMR90-4 iPSC-BMECs with or without exposure to Y-27632 at either time point (Fig. 4A, B). In addition, Western blotting for occludin, ZO-1, and claudin-5 protein at 2 days post-thaw revealed no changes in tight junction protein expression levels between cryopreserved BMECs with or without

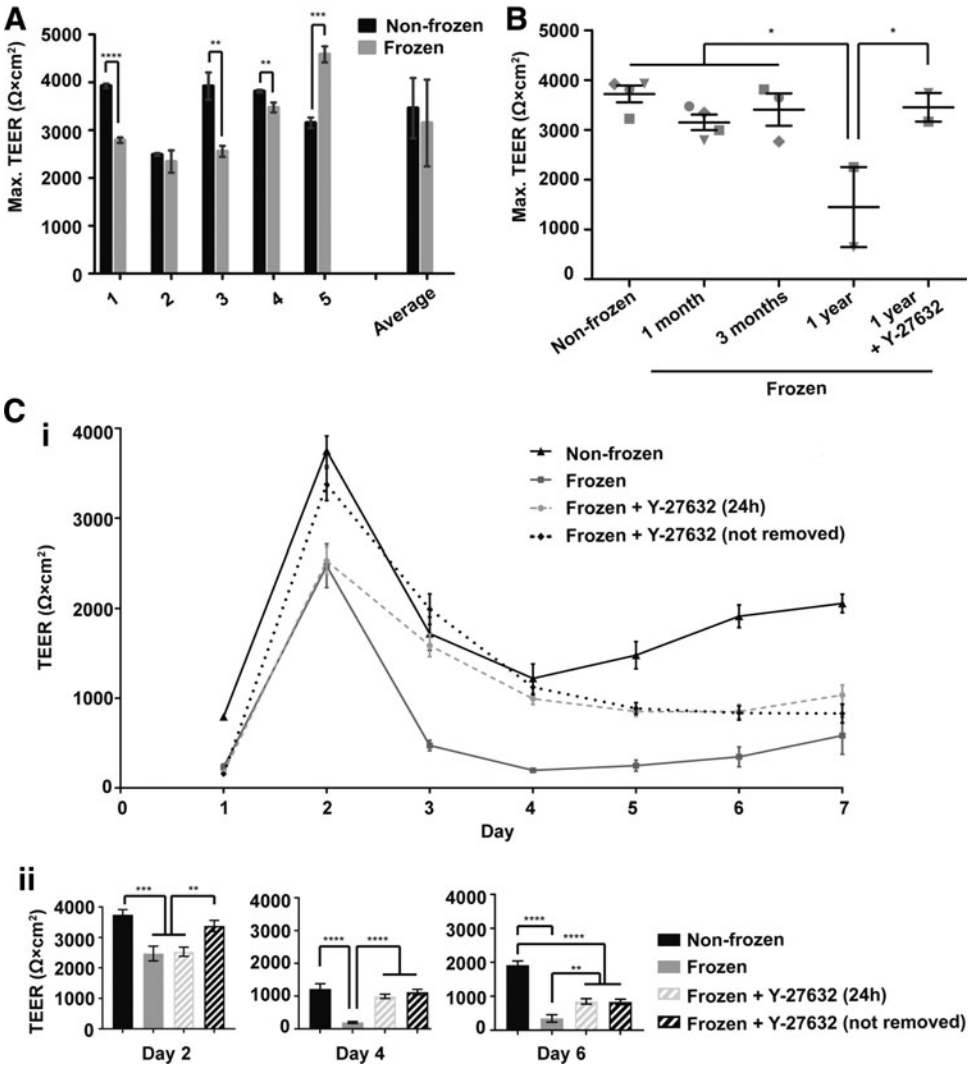

FIG. 3. TEER of D8 cryopreserved cells. **(A)** Maximum TEER values of IMR90-4 iPSC-BMECs cryopreserved at D8 of differentiation. TEER values from five independent differentiations are shown, with frozen and nonfrozen samples paired from the same independent differentiation. Maximum values were recorded at 48 h post-thaw for each sample. Data for differentiations one to five represent the average ± standard deviation of triplicate Transwell filters from a single independent differentiation. The average ± standard deviation of the five independent differentiations is also depicted. Statistical significance was calculated through Student's unpaired *t*-test (**$p < 0.01$, ***$p < 0.001$, ****$p < 0.0001$). **(B)** Maximum TEER of IMR90-4 iPSC-BMECs as a function of time in cryostorage. IMR90-4-derived cells were cryopreserved at D8 of differentiation and stored in liquid nitrogen for various lengths of time. Each data point represents the average maximum TEER value from triplicate filters from a single independent differentiation. Symbols indicate different independent differentiations. Statistical significance was calculated through ANOVA (*$p < 0.05$). **(C) (i)** TEER profile of IMR90-4 iPSC-BMECs cryopreserved at D8 of differentiation with or without 10 μM Y-27632 treatment. Data represent average ± standard deviation from triplicate Transwell filters from one independent differentiation, and the experiment was repeated for two additional differentiations to verify trends. **(ii)** TEER from days 2, 4, and 6 post-thaw. Data are derived from **(i)** and replotted here to depict the relevant statistical comparisons. Statistical significance was calculated through ANOVA (**$p < 0.01$, ***$p < 0.001$, ****$p < 0.0001$). TEER, transendothelial electrical resistance.

extended exposure to Y-27632 (Fig. 2B). Because Y-27632 can affect endothelial barrier function by modulating actin contractility through RhoA/ROCK signaling,[28] changes in actin cytoskeleton were next assessed. Interestingly, phalloidin staining of cryopreserved iPSC-BMECs at 4 days post-thaw showed an increase in stress fiber formation compared with nonfrozen cells that were eliminated by Y-27632 treatment (Fig. 4C). Thus, Y-27632 treatment can elevate the TEER of cryopreserved iPSC-BMECs and may do so by reducing stress fiber formation.

Discussion

In this study, we developed a method to cryopreserve iPSC-BMECs. It was determined that iPSC-BMECs could be cryopreserved at different differentiation stages, including D8, at which time the culture consists of a mixture of cell types, or alternatively at D10 when iPSC-BMECs have been purified and cultured for 2 days. In both cases, cryopreserved iPSC-BMECs retained BBB characteristics largely matching those of nonfrozen controls, including expression of endothelial

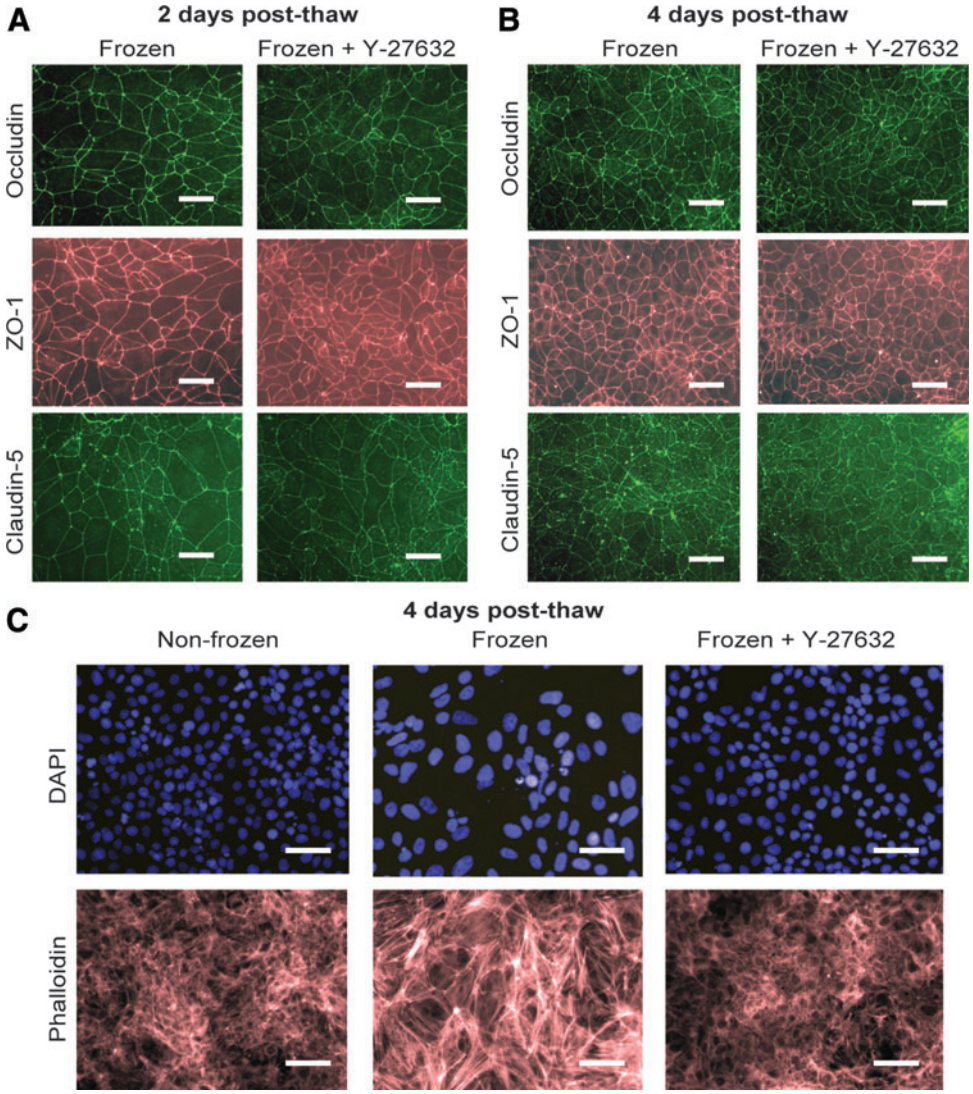

FIG. 4. Y-27632 prevents stress fiber formation in cryopreserved iPSC-BMECs. **(A)** IMR90-4 iPSC-BMECs were cryopreserved at D8 of differentiation and immunostained at D10, 2 days post-thaw. Y-27632 (10 μM) was present D8–D10. **(B)** IMR90-4 iPSC-BMECs were cryopreserved at D8 of differentiation and immunostained at D12, 4 days post-thaw. Y-27632 (10 μM) was present D8–D12. **(C)** IMR90-4 iPSC-BMECs were cryopreserved at D8 of differentiation, and phalloidin staining was performed at D12, 4 days post-thaw. Y-27632 (10 μM) was present D8–D12. **(A–C)** Scale bars, 50 μm. Color images available online at www.liebertpub.com/tec

and BBB markers, high TEER, and active efflux. However, freezing purified iPSC-BMECs at D10 resulted in a lower viable iPSC-BMEC yield than freezing the mixed cultures at D8 (10.6 vs. 20.1 BMECs per input iPSC, respectively). Thus, freezing at D8 is recommended over freezing at D10 as it results in roughly double the recovery of iPSC-BMECs for downstream experimental analyses without sacrificing BMEC purity. Using these cryopreservation approaches, the lead time to generate a purified iPSC-BMEC population is reduced from 13 days for a complete differentiation procedure to as a little as 1–2 days after thaw. Importantly, the iPSC-BMEC differentiation scheme itself is readily scalable,[25] and thus, expanded frozen stocks of iPSC-BMECs can be prevalidated and banked for use in large-scale screening or mechanistic studies.

In this protocol, we utilized ROCK inhibitor Y-27632 to improve iPSC-BMEC recovery following cryopreservation and to extend the elevated TEER profile of cryopreserved iPSC-BMECs. ROCK acts downstream of the small GTPase RhoA, which regulates cell adhesion and cytoskeletal dynamics.[29,30] In hPSCs, Y-27632 can prevent dissociation-induced apoptosis and thus improve cell viability during both routine passaging[31] as well as cryopreservation.[26,32] Y-27632 has further been used to aid recovery following cryopreservation of other cell types, including hPSC-derived cardiomyocytes[19,20] and hPSC-derived neural progenitors.[22] In this study, adding Y-27632 increased the iPSC-BMEC yield 1.9-fold from 20% ± 2% to 38% ± 5%, likely due to increased cell attachment of the cryopreserved cells.

Besides its use in hPSC culture, Y-27632 has been used extensively to probe involvement of RhoA/ROCK signaling in EC barrier function. At the BBB, Y-27632 has been shown to stabilize junctions and maintain BBB integrity in response to pathological conditions both *in vitro* and *in vivo*, such as invasion of metastatic lung cancer cells,[33] presence of HIV-infected monocytes,[34] and ischemic/reperfusion injury.[35] In particular, Y-27632 has been shown to prevent tight junction internalization,[33] and it can also prevent ROCK phosphorylation of claudin-5 and occludin,[34,36] which is associated with increased permeability.[37,38] In the iPSC-BMECs, 24 h Y-27632 treatment prolonged TEER elevation above 800 $\Omega \cdot cm^2$ out to 7 days post-thaw, and extended Y-27632 treatment additionally increased the maximum TEER at 48 h post-thaw. Despite the observed differences in TEER, Y-27632 treatment was not associated with any changes in the expression or localization of tight junction proteins occludin, claudin-5, or ZO-1. As a potential alternative explanation, activated ROCK

promotes the dynamic remodeling of the actin cytoskeleton in response to environmental stimuli such as soluble factors or physical forces, such that F-actin, which is normally distributed throughout the cytoplasm, assembles as stress fibers.[39] The stress fibers exert centripetal tension along the cell junctions as a result of myosin light chain (MLC)-dependent contraction, which physically disrupts cell junctions and increases permeability.[28,40] Inhibiting ROCK through Y-27632 blocks MLC-dependent actin–myosin contractility and stress fiber formation, thus promoting EC junctional stability,[28] which can be visualized through immunocytochemistry of EC junctions.[41] Stress fiber formation observed in cryopreserved iPSC-BMECs was prevented by Y-27632 treatment, suggesting that Y-27632 treatment may block junctional destabilization caused by cryopreservation-induced stress fiber formation. Finally, it is important to note that Y-27632 treatment was not necessary to achieve high TEER in cryopreserved iPSC-BMECs (e.g., Fig. 3A), although if longer duration of elevated TEER (≥3 days) is desired, then Y-27632 treatment is recommended for at least 24 h post-thaw.

Overall, iPSC-BMECs are becoming a more widespread cell source for human *in vitro* BBB models.[42,43] In this study, we have demonstrated that iPSC-BMECs can be cryopreserved for up to 1 year with Y-27632 supplementation post-thaw and retain BBB characteristics that rival nonfrozen iPSC-BMECs. We expect the methods developed here to greatly enhance the utility of the iPSC-BBB model, particularly for large-scale screening efforts.

Acknowledgments

The authors would like to thank Dr. Clive N. Svendsen and Dr. Gad D. Vatine for providing the CS03iCTRn2 iPSC line and the WiCell Research Institute for supplying reagents. This work was funded by NIH grant NS083688 (E.V.S. and S.P.P.), NIH Grant NS085351 (S.P.P. and E.V.S.), and the Takeda Pharmaceuticals New Frontier Science Program (E.V.S. and S.P.P.). H.K.W. was, in part, funded by a National Science Foundation (NSF) Graduate Research Fellowship.

Disclosure Statement

No competing financial interests exist.

References

1. Yang, Y., and Rosenberg, G.A. Blood-brain barrier breakdown in acute and chronic cerebrovascular disease. Stroke **42,** 3323, 2011.
2. Shlosberg, D., Benifla, M., Kaufer, D., and Friedman, A. Blood-brain barrier breakdown as a therapeutic target in traumatic brain injury. Nat Rev Neurol **6,** 393, 2010.
3. Zlokovic, B.V. Neurovascular pathways to neurodegeneration in Alzheimer's disease and other disorders. Nat Rev Neurosci **12,** 723, 2011.
4. Pardridge, W.M. The blood-brain barrier: bottleneck in brain drug development. NeuroRx **2,** 3, 2005.
5. Tietz, S., and Engelhardt, B. Brain barriers: crosstalk between complex tight junctions and adherens junctions. J Cell Biol **209,** 493, 2015.
6. Begley, D.J. ABC transporters and the blood-brain barrier. Curr Pharm Des **10,** 1295, 2004.
7. Tsuji, A. Small molecular drug transfer across the blood-brain barrier via carrier-mediated transport systems. NeuroRx **2,** 54, 2005.
8. Weksler, B.B., Subileau, E.A., Perriere, N., Charneau, P., Holloway, K., Leveque, M., Tricoire-Leignel, H., Nicotra, A., Bourdoulous, S., Turowski, P., Male, D.K., Roux, F., Greenwood, J., Romero, I.A., and Couraud, P.O. Blood-brain barrier-specific properties of a human adult brain endothelial cell line. FASEB J **19,** 1872, 2005.
9. Navone, S.E., Marfia, G., Invernici, G., Cristini, S., Nava, S., Balbi, S., Sangiorgi, S., Ciusani, E., Bosutti, A., Alessandri, G., Slevin, M., and Parati, E.A. Isolation and expansion of human and mouse brain microvascular endothelial cells. Nat Protoc **8,** 1680, 2013.
10. Lippmann, E.S., Azarin, S.M., Kay, J.E., Nessler, R.A., Wilson, H.K., Al-Ahmad, A., Palecek, S.P., and Shusta, E.V. Derivation of blood-brain barrier endothelial cells from human pluripotent stem cells. Nat Biotechnol **30,** 783, 2012.
11. Lippmann, E.S., Al-Ahmad, A., Azarin, S.M., Palecek, S.P., and Shusta, E.V. A retinoic acid-enhanced, multicellular human blood-brain barrier model derived from stem cell sources. Sci Rep **4,** 4160, 2014.
12. Boyer-Di Ponio, J., El-Ayoubi, F., Glacial, F., Ganeshamoorthy, K., Driancourt, C., Godet, M., Perriere, N., Guillevic, O., Couraud, P.O., and Uzan, G. Instruction of circulating endothelial progenitors in vitro towards specialized blood-brain barrier and arterial phenotypes. PLoS One **9,** e84179, 2014.
13. Cecchelli, R., Aday, S., Sevin, E., Almeida, C., Culot, M., Dehouck, L., Coisne, C., Engelhardt, B., Dehouck, M.P., and Ferreira, L. A stable and reproducible human blood-brain barrier model derived from hematopoietic stem cells. PLoS One **9,** e99733, 2014.
14. Robertson, P.L., Du Bois, M., Bowman, P.D., and Goldstein, G.W. Angiogenesis in developing rat brain: an in vivo and in vitro study. Brain Res **355,** 219, 1985.
15. Bernas, M.J., Cardoso, F.L., Daley, S.K., Weinand, M.E., Campos, A.R., Ferreira, A.J., Hoying, J.B., Witte, M.H., Brites, D., Persidsky, Y., Ramirez, S.H., and Brito, M.A. Establishment of primary cultures of human brain microvascular endothelial cells to provide an in vitro cellular model of the blood-brain barrier. Nat Protoc **5,** 1265, 2010.
16. Smith, M., Omidi, Y., and Gumbleton, M. Primary porcine brain microvascular endothelial cells: biochemical and functional characterisation as a model for drug transport and targeting. J Drug Target **15,** 253, 2007.
17. Zhang, Y., Li, C.S., Ye, Y., Johnson, K., Poe, J., Johnson, S., Bobrowski, W., Garrido, R., and Madhu, C. Porcine brain microvessel endothelial cells as an in vitro model to predict in vivo blood-brain barrier permeability. Drug Metab Dispos **34,** 1935, 2006.
18. Brandl, C., Zimmermann, S.J., Milenkovic, V.M., Rosendahl, S.M., Grassmann, F., Milenkovic, A., Hehr, U., Federlin, M., Wetzel, C.H., Helbig, H., and Weber, B.H. In-depth characterisation of Retinal Pigment Epithelium (RPE) cells derived from human induced pluripotent stem cells (hiPSC). Neuromolecular Med **16,** 551, 2014.
19. Kim, Y.Y., Ku, S.Y., Liu, H.C., Cho, H.J., Oh, S.K., Moon, S.Y., and Choi, Y.M. Cryopreservation of human embryonic stem cells derived-cardiomyocytes induced by BMP2 in serum-free condition. Reprod Sci **18,** 252, 2011.
20. Xu, C., Police, S., Hassanipour, M., Li, Y., Chen, Y., Priest, C., O'Sullivan, C., Laflamme, M.A., Zhu, W.Z., Van Biber,

B., Hegerova, L., Yang, J., Delavan-Boorsma, K., Davies, A., Lebkowski, J., and Gold, J.D. Efficient generation and cryopreservation of cardiomyocytes derived from human embryonic stem cells. Regen Med **6,** 53, 2011.
21. Chong, J.J., Yang, X., Don, C.W., Minami, E., Liu, Y.W., Weyers, J.J., Mahoney, W.M., Van Biber, B., Cook, S.M., Palpant, N.J., Gantz, J.A., Fugate, J.A., Muskheli, V., Gough, G.M., Vogel, K.W., Astley, C.A., Hotchkiss, C.E., Baldessari, A., Pabon, L., Reinecke, H., Gill, E.A., Nelson, V., Kiem, H.P., Laflamme, M.A., and Murry, C.E. Human embryonic-stem-cell-derived cardiomyocytes regenerate nonhuman primate hearts. Nature **510,** 273, 2014.
22. Nemati, S., Hatami, M., Kiani, S., Hemmesi, K., Gourabi, H., Masoudi, N., Alaei, S., and Baharvand, H. Long-term self-renewable feeder-free human induced pluripotent stem cell-derived neural progenitors. Stem Cells Dev **20,** 503, 2011.
23. Stebbins, M.J., Wilson, H.K., Canfield, S.G., Qian, T., Palecek, S.P., and Shusta, E.V. Differentiation and characterization of human pluripotent stem cell-derived brain microvascular endothelial cells. Methods **101,** 93, 2016.
24. Yu, J., Vodyanik, M.A., Smuga-Otto, K., Antosiewicz-Bourget, J., Frane, J.L., Tian, S., Nie, J., Jonsdottir, G.A., Ruotti, V., Stewart, R., Slukvin, II, and Thomson, J.A. Induced pluripotent stem cell lines derived from human somatic cells. Science **318,** 1917, 2007.
25. Wilson, H.K., Canfield, S.G., Hjortness, M.K., Palecek, S.P., and Shusta, E.V. Exploring the effects of cell seeding density on the differentiation of human pluripotent stem cells to brain microvascular endothelial cells. Fluids Barriers CNS **12,** 13, 2015.
26. Claassen, D.A., Desler, M.M., and Rizzino, A. ROCK inhibition enhances the recovery and growth of cryopreserved human embryonic stem cells and human induced pluripotent stem cells. Mol Reprod Dev **76,** 722, 2009.
27. Miyazaki, T., Nakatsuji, N., and Suemori, H. Optimization of slow cooling cryopreservation for human pluripotent stem cells. Genesis **52,** 49, 2014.
28. Spindler, V., Schlegel, N., and Waschke, J. Role of GTPases in control of microvascular permeability. Cardiovasc Res **87,** 243, 2010.
29. Watanabe, T., Sato, K., and Kaibuchi, K. Cadherin-mediated intercellular adhesion and signaling cascades involving small GTPases. Cold Spring Harb Perspect Biol **1,** a003020, 2009.
30. Popoff, M.R., and Geny, B. Multifaceted role of Rho, Rac, Cdc42 and Ras in intercellular junctions, lessons from toxins. Biochim Biophys Acta **1788,** 797, 2009.
31. Watanabe, K., Ueno, M., Kamiya, D., Nishiyama, A., Matsumura, M., Wataya, T., Takahashi, J.B., Nishikawa, S., Nishikawa, S., Muguruma, K., and Sasai, Y. A ROCK inhibitor permits survival of dissociated human embryonic stem cells. Nat Biotechnol **25,** 681, 2007.
32. Li, X., Krawetz, R., Liu, S., Meng, G., and Rancourt, D.E. ROCK inhibitor improves survival of cryopreserved serum/feeder-free single human embryonic stem cells. Hum Reprod **24,** 580, 2009.
33. Li, B., Zhao, W.D., Tan, Z.M., Fang, W.G., Zhu, L., and Chen, Y.H. Involvement of Rho/ROCK signalling in small cell lung cancer migration through human brain microvascular endothelial cells. FEBS Lett **580,** 4252, 2006.
34. Persidsky, Y., Heilman, D., Haorah, J., Zelivyanskaya, M., Persidsky, R., Weber, G.A., Shimokawa, H., Kaibuchi, K., and Ikezu, T. Rho-mediated regulation of tight junctions during monocyte migration across the blood-brain barrier in HIV-1 encephalitis (HIVE). Blood **107,** 4770, 2006.
35. Shi, Y., Zhang, L., Pu, H., Mao, L., Hu, X., Jiang, X., Xu, N., Stetler, R.A., Zhang, F., Liu, X., Leak, R.K., Keep, R.F., Ji, X., and Chen, J. Rapid endothelial cytoskeletal reorganization enables early blood-brain barrier disruption and long-term ischaemic reperfusion brain injury. Nat Commun **7,** 10523, 2016.
36. Yamamoto, M., Ramirez, S.H., Sato, S., Kiyota, T., Cerny, R.L., Kaibuchi, K., Persidsky, Y., and Ikezu, T. Phosphorylation of claudin-5 and occludin by rho kinase in brain endothelial cells. Am J Pathol **172,** 521, 2008.
37. Haorah, J., Knipe, B., Leibhart, J., Ghorpade, A., and Persidsky, Y. Alcohol-induced oxidative stress in brain endothelial cells causes blood-brain barrier dysfunction. J Leukoc Biol **78,** 1223, 2005.
38. Hirase, T., Kawashima, S., Wong, E.Y., Ueyama, T., Rikitake, Y., Tsukita, S., Yokoyama, M., and Staddon, J.M. Regulation of tight junction permeability and occludin phosphorylation by Rhoa-p160ROCK-dependent and -independent mechanisms. J Biol Chem **276,** 10423, 2001.
39. Burridge, K., and Wittchen, E.S. The tension mounts: stress fibers as force-generating mechanotransducers. J Cell Biol **200,** 9, 2013.
40. Vandenbroucke, E., Mehta, D., Minshall, R., and Malik, A.B. Regulation of endothelial junctional permeability. Ann N Y Acad Sci **1123,** 134, 2008.
41. Millan, J., Cain, R.J., Reglero-Real, N., Bigarella, C., Marcos-Ramiro, B., Fernandez-Martin, L., Correas, I., and Ridley, A.J. Adherens junctions connect stress fibres between adjacent endothelial cells. BMC Biol **8,** 11, 2010.
42. Wang, Y.I., Abaci, H.E., and Shuler, M.L. Microfluidic blood-brain barrier model provides in vivo-like barrier properties for drug permeability screening. Biotechnol Bioeng 2016; [Epub ahead of print], doi: 10.1002/bit.26045.
43. Katt, M.E., Xu, Z.S., Gerecht, S., and Searson, P.C. Human brain microvascular endothelial cells derived from the BC1 iPS cell line exhibit a blood-brain barrier phenotype. PLoS One **11,** e0152105, 2016.

Address correspondence to:
Eric V. Shusta, PhD
Department of Chemical and Biological Engineering
University of Wisconsin-Madison
1415 Engineering Drive
Madison, WI 53706

E-mail: shusta@engr.wisc.edu

Sean P. Palecek, PhD
Department of Chemical and Biological Engineering
University of Wisconsin-Madison
1415 Engineering Drive
Madison, WI 53706

E-mail: palecek@engr.wisc.edu

Received: August 24, 2016
Accepted: November 14, 2016
Online Publication Date: December 12, 2016